ISSN: 1696-8352

Mechanistic study of lodenafil carbonate electrochemical reduction in acid medium

Estudo mecânico da redução eletroquímica do carbonato de lodenafil em meio ácido

DOI: 10.55905/oelv21n8-077

Recebimento dos originais: 17/07/2023
Aceitação para publicação: 15/08/2023

Jonatas Schadeck Carvalho
Master in Applied Chemistry
Institution: Universidade Estadual do Centro-Oeste (UNICENTRO)
Address: Alameda Élio Antonio Dalla Vecchia, 838, Vila Carli, Guarapuava – PR, CEP: 85040-167
E-mail: jonatas-goio@hotmail.com

Andressa Galli
Doctor of Science
Institution: Universidade Estadual do Centro-Oeste
Address: Alameda Élio Antonio Dalla Vecchia, 838, Vila Carli, Guarapuava – PR, CEP: 85040-167
E-mail: andressagalli@gmail.com

Sergio Antonio Spinola Machado
Doctor of Science
Institution: Instituto de Química de São Carlos da Universidade de São Paulo (IQSC-USP)
Address: Av. Trabalhador São-Carlense, 400, São Carlos – SP, CEP: 13566-590
E-mail: sasmach@iqsc.usp.br

Sueli Pércio Quináia
Doctor of Science
Institution: Universidade Estadual do Centro-Oeste (UNICENTRO)
Address: Alameda Élio Antonio Dalla Vecchia, 838, Vila Carli, Guarapuava – PR, CEP: 85040-167
E-mail: spquinaia@unicentro.br

ISSN: 1696-8352

ABSTRACT
The electrochemical reduction mechanism of lodenafil carbonate in acidic medium was studied using cyclic voltammetry, square wave voltammetry and chronoamperometry (sulfuric acid 0.1 mol L^{-1}, potential controlled at -1.2 V). The formed product characterization was carried out by FT-IR spectroscopy combined with quantum calculations of the lodenafil molecular orbitals. Over the products IR spectrum, it was possible to note the presence of absorption bands corresponding to the aldehyde, amine and ethanol groups. These results, together with those obtained by electrochemical techniques and quantum calculations, allowed us to propose that the process of reducing lodenafil is dependent on protons and occurs in four irreversible steps, the first being the amide group reduction to an aldehyde and a primary amine. Then, the aldehyde is reduced to an alcohol, with the consumption of two electrons and two protons in each of these steps. Then, there is a reduction in two processes of one electron and one proton each, one of which by a radical way. In this last process, there are two possibilities: one is the sulfone group reduction and the other is the azomethine reduction adjacent to the amine group formed in the previous step.

Keywords: lodenafil carbonate, electrochemical reduction, mercury electrode, dft calculations.

RESUMO
O mecanismo de redução eletroquímica do carbonato de lodenafil em meio ácido foi estudado usando voltametria cíclica, voltametria de onda quadrada e cronoamperometria (ácido sulfúrico 0,1 mol L-1, potencial controlado a -1,2 V). A caracterização do produto formado foi realizada por espectroscopia FT-IR combinada com cálculos quânticos dos orbitais moleculares de lodenafil. Sobre o espectro IR produtos, foi possível notar a presença de bandas de absorção correspondentes aos grupos aldeído, amina e etanol. Esses resultados, juntamente com os obtidos por técnicas eletroquímicas e cálculos quânticos, permitiram propor que o processo de redução do lodenafil seja dependente de prótons e ocorra em quatro etapas irreversíveis, sendo a primeira a redução do grupo amida a aldeído e a amina primária. Em seguida, o aldeído é reduzido a um álcool, com o consumo de dois elétrons e dois prótons em cada um desses passos. Em seguida ocorre a redução de dois processos de um elétron e de um próton cada, sendo que um por via radical. Neste último processo, há duas possibilidades: uma é a redução do grupo sulfona e a outra é a redução de azometina adjacente ao grupo amina formado no passo anterior.

Palavras-chave: carbonato de lodenafil, redução eletroquímica, eletrodo de mercúrio, cálculos de dft.

1 INTRODUCTION

Lodenafil carbonate (LC), a drug developed in Brazil, it is used to treat erectile dysfunction and consists of a dimer formed by two lodenafil molecules connected by a

ISSN: 1696-8352

carbonate bridge (Figure 1) (Alshehri et al, 2022; Scaglione et al, 2017; Davis et al, 2012; Codervilla et al, 2013). After ingestion, the carbonate bridge is broken, releasing two molecules of lodenafil. Then, this one will act selectively by inhibiting the action of the phosphodiesterase type 5 enzyme (PDE-5). This enzyme is responsible for the guanosine monophosphate cyclic (GMPc), hydrolysis. The GMPc relaxes the smooth muscle of the penis cavernous body. This increases blood flow in the region. As lodenafil hinders the action of PDE-5 and consequently the GMPc degradation, it maintains GMPc concentration, which facilitates the maintenance of penile erection (Davis et al, 2012; Codervilla et al, 2013).

Figure 1. Chemical structures of lodenafil carbonate (a) and lodenafil (b).

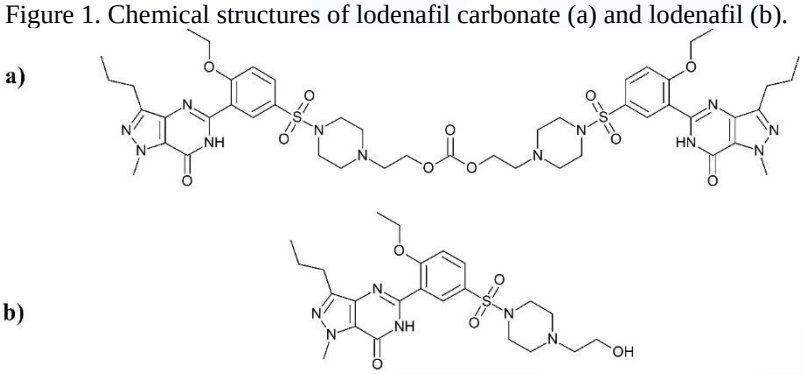

Source: Author

Although voltammetric methods have been developed to PDE-5 inhibitors determination, the electrochemical reduction mechanism of these drugs is not yet known. Thus, some studies have been carried out in an attempt to elucidate the electrochemical mechanism of these molecules. Berzas *et al.* (2000) studied the electrochemical behavior of the sildenafil molecule in $HClO_4$ (pH 2) on the hanging mercury drop electrode (HMDE), while Uslu *et al.* (2005) evaluated the electrochemical behavior of vardenafil on the glassy carbon electrode in an acid medium (Berzas et al, 2000; Uslu et al, 2005). In both studies, the reversibility of the respective reactions was not observed and it was proposed that the reduction or oxidation of the studied molecules should occur in the piperazine ring (Berzas et al, 2000; Uslu et al, 2005). Han *et al.* (2012) studied the electrochemical behavior of udenafil on the glassy carbon electrode in an acid medium. They observed that, under these conditions, udenafil is irreversible oxidized and oxidation has been

ISSN: 1696-8352

proposed to occur in the alkoxybenzene and 6-hydroxipurine groups (Han et al, 2012). However, the mechanistic propositions of PDE-5 inhibitor drugs were based exclusively on voltammetry, which provides limited data on the mechanism (Berzas et al, 2000; Uslu et al, 2005; Han et al, 2012). One way to obtain reliable mechanistic data is over the use of controlled potential electrolysis, with the characterization of the products formed (Galli et al, 2018). In addition, the quantum properties of the molecules can be obtained using software (for example ORCA®), which allows identifying the region most susceptible to reduce or oxidize, being a useful tool in mechanistic studies (Galli et al, 2018; Marrani et al, 2019).

Considering that, the electrochemical mechanism of PDE-5 inhibitors has not been fully discussed. In this work, LC was used as a model molecule to investigate the reduction mechanism of PDE-5 inhibitors in acid medium. For this, studies were carried out by voltammetry, controlled potential electrolysis, with the characterization of products formed by FT-IR spectroscopy, in addition to quantum calculations performed in the ORCA® software.

2 EXPERIMENTAL

2.1 INSTRUMENTS AND SOLUTIONS

All reagents used were of analytical grade. Nitrogen (Air Liquide, 99.999%) was used as a purge gas. The LC standard solution (0.101 mmol L^{-1}) was prepared with the complete dissolution of the standard LC (Cristália Produtos Químicos Farmacêuticos, 98.6%) in 500.0 µL of dichloromethane (Nuclear, 99.5%), followed by addition of ethanol (FMaia, 95.0%) until the volume of 10.0 mL. Sulfuric acid solutions were prepared by dissolving the concentrated acid (H_2SO_4, Merk, 95-97%) in ultrapure water obtained by the Milli-Q® system (Millipore, Brazil). All solutions were prepared on the same day of analysis and used in voltammetric techniques and electrolysis. For infrared measurements, potassium bromide (KBr, Sigma-Aldrich, 99%) with FT-IR grade was used.

Voltammetric measurements were performed with a Metrohm® 747 VA voltammetric analyzer coupled to an electrochemical cell composed of three electrodes:

ISSN: 1696-8352

working electrode (HMDE, drop size 4), Ag/AgCl reference electrode (KCl 3.0 mol L^{-1}) and a platinum wire as the auxiliary electrode. Ultraviolet (UV) spectrophotometry measurements were performed on an AvaSpec-2048® spectrometer. In addition, the reagent and the product characterizations were performed by FT-IR spectroscopy in an infrared spectrophotometer with Fourier transform Shimadzu IRAffinity 1®.

Electrolysis with controlled potential was performed in an Autolab® potentiostat, using a cell with three electrodes, namely: mercury pool electrode (working electrode), Ag/AgCL electrode in KCl 3.0 mol L^{-1} (reference electrode) and a platinum sheet 1 cm^2 (auxiliary electrode). This cell has two compartments, each with 40 mL capacity, joined by a glass junction with a sintered glass membrane between the junction and the outlets of each compartment. The N_2 gas was used to bubble the system and remove dissolved O_2 from the medium.

2.2 VOLTAMMETRIC MEASUREMENTS

To evaluate the electrochemical behavior of the LC on the HMDE, measurements were performed by cyclic voltammetry performed in a cell containing 10 ml of a solution (LC 0.7 µmol L^{-1} and H_2SO_4 0.1 mol L^{-1}). This study was carried out by increasing the scan rate (v), keeping the other parameters fixed. The scan rate was varied from 25 to 300 mV s^{-1}, and the fixed parameters were accumulation time (t_{ac}) 30 s and accumulation potential (E_{ac}) -0.8 V. Then, the square wave voltammetry technique was used to obtain data on the LC reduction mechanism and to estimate the number of electrons involved in each reaction step. In this study, the frequency of application of potential pulses varied from 10 to 140 Hz, keeping the other parameters constant, that is, t_{ac} 30 s, E_{ac} -0.8 V, equilibration time (t_{eq}) 10 s, scan increment (ΔE_s) 6 mV, amplitude (a) 40 mV, and 120 Hz frequency (f). This study was carried out in a 10 mL cell containing solutions of LC 1.2 µmol L^{-1} in H_2SO_4 0.1 mol L^{-1}.

ISSN: 1696-8352

2.3 CONTROLLED POTENTIAL ELECTROLYSIS

For the LC electrolysis, 20.0 ml of LC solution (50.0 µmol L^{-1}) in H_2SO_4 0.1 mol L^{-1} medium was added to each cell container. The controlled potential electrolysis occurred at -1.2 V, ensuring the occurrence of all reduction processes.

2.4 UV MEASUREMENTS

Before and after each electrolysis, aliquots from the reduction compartment were analyzed by UV at wavelengths from 200 nm to 800 nm and, after the measurement, these aliquots were returned to the electrolysis compartment.

2.5 CHARACTERIZATIONS BY FT-IR SPECTROSCOPY

After electrolysis, the formed products were extracted three times with 25.0 mL of dichloromethane. Then, the samples were dried with anhydrous sodium sulfate (Na_2SO_4, Sigma-Aldrich, 99%), filtered and the solvent evaporated at room temperature. Then, the samples were left in a desiccator with a vacuum for 24 hours. After drying, the samples were characterized by FT-IR using pellets produced with KBr and the LC or the sample obtained after electrolysis.

2.6 CHEMICAL-QUANTUM CALCULATIONS

Chemical-quantum calculations were performed in the ORCA® 4.0.1 software package (Neese, 2012). Structural relaxation occurred using the density functional theory method (DFT). For this purpose, the base function def2-TVZP(-f) (who acts with the removal of the f orbitals) was used together with the functional hybrid B3LYP [7]. To speed up the calculations, integration by chain of spheres (RIJCOSX) was used together with the auxiliary function for Coulomb integral (def2/J), integration gradient and calculation constrained in 6 (Grid 6 and GridX 6), without final constriction for energy calculation (NoFinalGrid). (Neese, 2012). HOMO and LUMO molecular orbitals were rendered in the Avogadro® 1.2.0 program (Hanwell et al, 2012). For the isosurfaces construction of all orbitals, a value of 0.02 atomic units was used (Galli et al, 2018).

ISSN: 1696-8352

3 RESULTS AND DISCUSSION

3.1 MECHANISM STUDIES BY VOLTAMMETRIC TECHNIQUES

Cyclic voltammetry was used to evaluate the nature of the reduction process of LC. Figure 2 shows the cyclic voltammograms of LC as a function of scan rate variation. It is possible to notice the presence of three peaks, the first at -0.9 V, the second near -1.0 V and the last at -1.1 V. However, the third peak is only visible from 150 mV s^{-1}, probably due to high process speed. There are no peaks in the reverse direction of scan and the peaks potential shifts to more cathodic regions with scan rate increases, indicating that the process occurs irreversibly (Wang, 2006).

Figure 2. Complete cyclic voltammograms of LC 0.700 µmol L-1 in H2SO4 0.1 mol L-1, with different scan rate. Voltammetric conditions: Eac -0.8 v; tac 30 s; teq 10 s; ΔEs 6 mv s^{-1}.

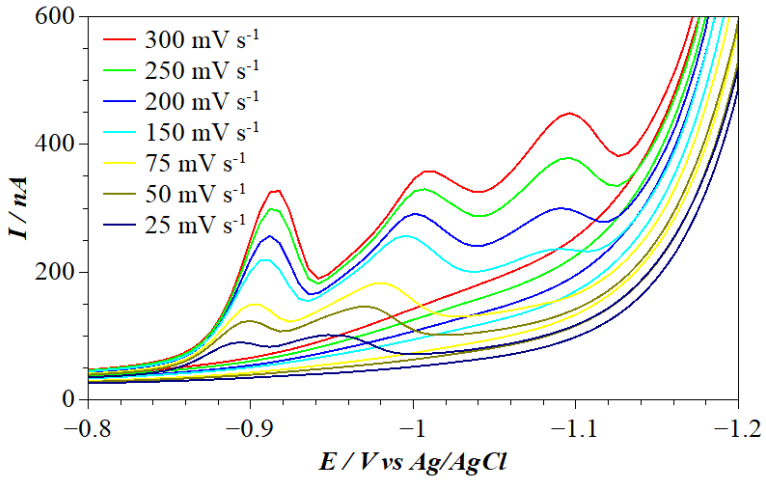

Source: Author.

The data indicate that the first (-0.9 V) and second (-1.0 V) LC reduction processes occur with speed control by diffusion, as they have a non-linear relationship between the peak current (I_P) and the scan rate (v) (Supplementary Material, Fig. S1). There is also a linear relationship between log I_P and log v (Supplementary Material, Fig. S2), with slope coefficients equal to 0.526 for the first and 0.506 for the second peak, as well as a linear relationship between I_P and $v^{1/2}$ (Supplementary Material, Fig. S3). In turn, the third process (-1.1 V) showed characteristics of reactions controlled by electronic transfer, as it has a linear relationship between I_P and v (Supplementary Material, Fig. S1) and

ISSN: 1696-8352

between log I_P and log v (Supplementary Material, Fig. S2) with slope equal to 0.998, in addition to a non-linear relationship between I_P and $v^{1/2}$ (Supplementary Material, Fig. S3). This indicates that this last step occurs with the product of the previous reactions, which would also explain the irreversibility of the reaction since the initial product is being chemically "removed" from the electrode surface (Gosser-Junior, 1993; Bard, Faulkner, 2001). To obtain more information on the reduction mechanism, square wave voltammetry analyzes were performed. The data obtained with the variation in the frequency of application of the potential pulses (f) demonstrate the presence of four reduction peaks. One more than was perceptible by cyclic voltammetry. This peak is probably due to a reduction process that occurs faster than cyclic voltammetry can register. It is also noted that there is a change in peak potentials for more negative regions with an increase in frequency (Figure 3a), in addition to the fact that both peaks have a linear relationship between I_P and f (Figure 3b). These data are consistent with irreversible processes and with the data obtained by cyclic voltammetry (Souza, 2003).

Figure 3. (a) square wave voltammograms (LC 1.2 µmol L-1) at different frequencies. (b) Relationship between the peak current and the frequency. Voltammetric conditions: Eac -0.8 V; tac 30 s; teq 10 s; α 40 mV; ΔES 6 mV s^{-1}.

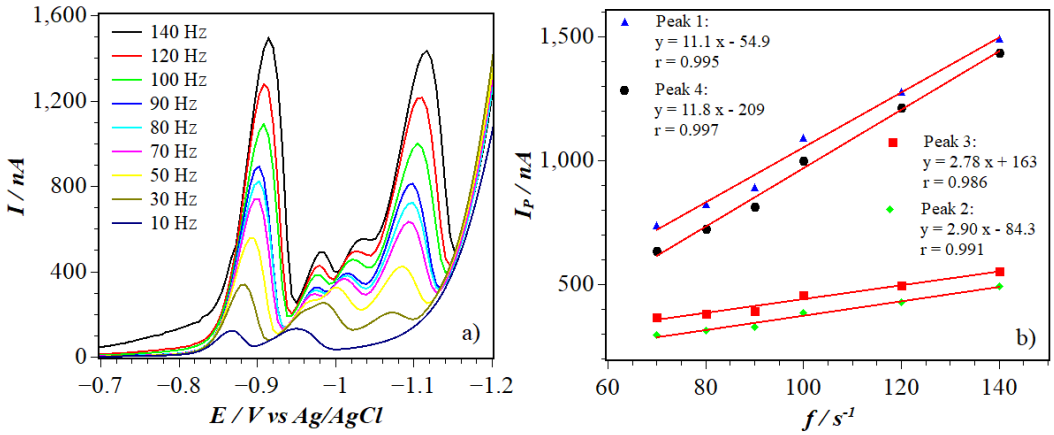

Source: Author.

A linearity relationship between the peak potential (E_P) as a function of the variation of the frequency logarithm is characteristic of totally irreversible reactions, represented by Equation 1 (Souza, 2003). Where E_P is the peak potential, f is the

ISSN: 1696-8352

frequency, R is the ideal gas constant, T is the temperature, α is the electron transfer coefficient, n is the number of electrons involved in the reaction and F is the Faraday constant (Souza, 2003; Skoog et al, 2013).

$$\frac{\Delta E_P}{\Delta log f} = \frac{-2{,}3RT}{\alpha nF} (Equation 1)$$

With the data obtained by the square wave voltammetry frequency variation, it was possible to perform a linear regression between ΔE_P and $\Delta log f$. This regression provided the values of the slope coefficient, which were applied in Equation 1 and, considering α = 0.5, it was possible to estimate the number of electrons involved in the reaction rate determinant step for each of the processes (Table 1) (Gosser-Junior, 1993).

Table 1. Estimation of electrons number for the LC reduction

	Slope coefficient	Calculated n	Approximate n
Peak 1	-0.0450	2.63	3
Peak 2	-0.0266	4.45	5
Peak 3	-0.0679	1.74	2
Peak 4	-0.0604	1.96	2
Total		**10.79**	**12**

Source: Author.

However, α value corresponds to a measure of the symmetry of the activation energy barrier so that the electronic transfer occurs, staying between 0 and 1. In general, for metallic conductors the value of 0.5 is assumed, because in this situation the activated complex is in an intermediate region between reagents and products, presenting characteristics of oxidized and reduced species. However, α may change due to secondary reactions or adsorption processes, so 0.5 may not be the most appropriate value. Thus, the electron number obtained need to be proven by controlled potential electrolysis (Bard, Faulkner, 2001, Brett, Brett, 1993).

3.2 CONTROLLED POTENTIAL ELECTROLYSIS

Figure 4 shows that there was an exponential decay of the current with 2 hours of electrolysis, indicating the consumption of the analyte and consequent product formation.

ISSN: 1696-8352

It was possible to note the presence of two peaks (30 and 60 min) that refer to the pause in electrolysis to remove the aliquot to perform the UV spectrometry measurements.

Figure 4. Chronoamperogram (LC 50.0 µmol L-1, sulfuric acid 0.1 mol L-1, potential controlled at -1.2 V).

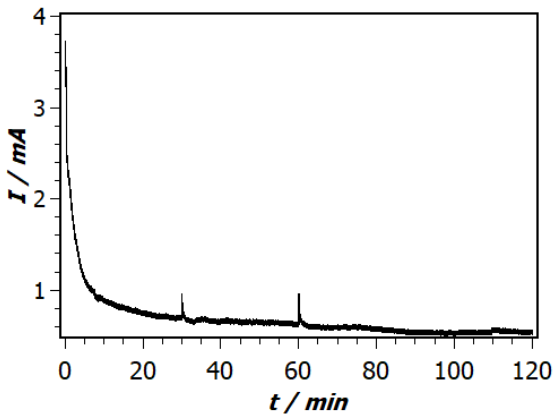

Source: Author.

To monitor the drop in the analytical signal, UV measurements were performed before and after each electrolysis (Figure 5. It was possible to observe the decay of absorption, which confirms the LC consumption and the formation of products over the time of electrolysis. In addition, there is no peak formation in another region of the spectrum, indicating that the reaction products do not absorb in the region of 200 to 800 nm.

Figure 5. LC (50.0 µmol L-1) UV spectrum at different electrolysis times.

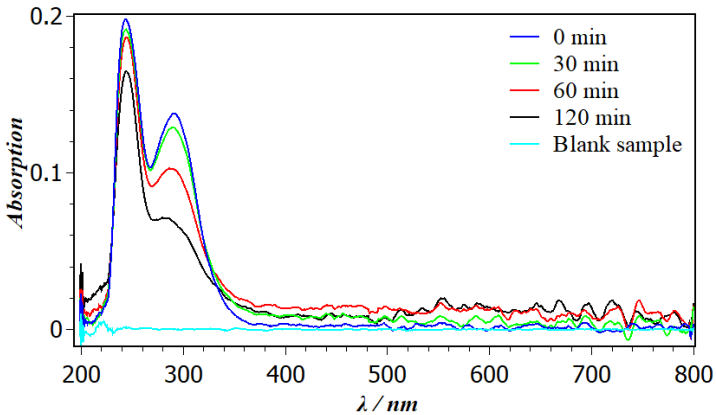

Source: Author.

The chronoamperogram integration provided the value of the charge (Q) consumed during electrolysis, so that, with the data obtained, it was possible to calculate the number of moles of reagent consumed in the LC reduction. These values were applied in Equation 2, where Q = charge, n = number of electrons, F = Faraday constant and N the number of moles of reagent consumed. Thus, the number of electrons involved in the global reaction was calculated at 10.82 for peak 1 (absorption at 245 nm) and 5.53 for peak 2 (absorption at 290 nm). These different results indicate that there are probably two processes occurring independently and at different speeds, one of them occurs with the region of the molecule that absorbs at 245 nm and the other occurs in the region of the molecule that absorbs at 290 nm. It is observed that the electron value found, considering the first peak (10.82), is very close to that found by the square wave voltammetry (10.79), therefore this value was considered the truth. $Q = nFN (Equation 2)$

3.3 INFRARED SPECTROSCOPY CHARACTERIZATIONS

Figure 6 shows the infrared absorption spectrum of LC, as well as its chemical structure with the indication of the regions of the molecule that originate the main absorption bands, and Table 2 shows the possible assignments of each absorption band.

Figure 6. Infrared absorption spectrum of LC.

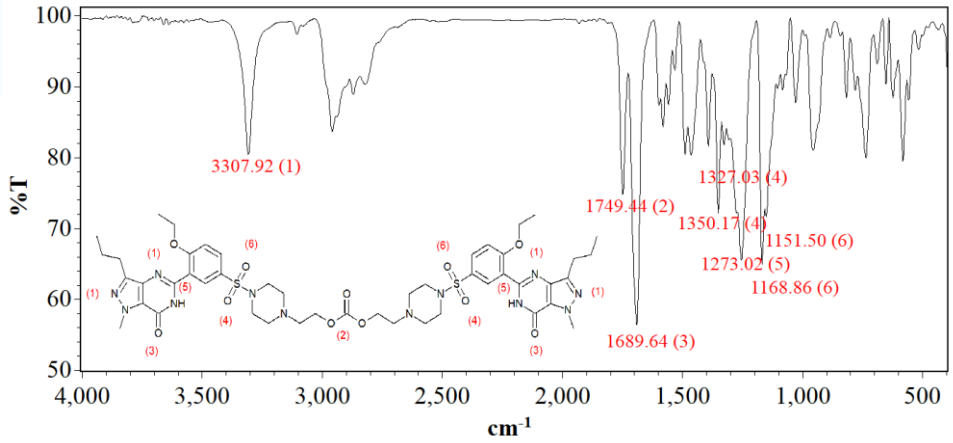

Source: Author.

ISSN: 1696-8352

Table 2. Absorption frequencies and assignments of LC main absorption bands in the infrared.

Wavenumber	Possible assignments [18,19]
3307.92	Secondary amine axial stretching
1749.44	C=O axial stretching (aliphatic ester)
1689.64	C=O axial stretching (amide)
1350.17 e 1327.03	S=O asymmetric axial stretching (sulfone)
1273.02	C-N axial stretching (aromatic amine)
1168.86 e 1151.50	S=O symmetric axial stretching (sulfone)

Source: Author.

FT-IR analyzes were also performed with the product obtained. The product infrared absorption spectrum and the main absorption bands with the possible assignments are represented, respectively, in Figure 7 and Table 3. It was observed that, after electrolysis, the sample had an infrared spectrum with significant differences compared to the standard LC, confirming changes in the structure of the molecule. A wideband appeared at 3396 cm^{-1}, characteristic of the O-H stretch of alcohol, which generally covers the bands corresponding to the axial deformation of the amines, such as the one present in the LC spectrum. There is also an absorption at 1637 cm^{-1}, due to the N-H bending for primary amine, since absorption occurs closer to 1640 cm^{-1}, in contrast to the secondary amines absorption that occurs close to 1500 cm^{-1} (Pavia, 2009).

Figure 7. Infrared absorption spectrum of the sample after electrolysis.

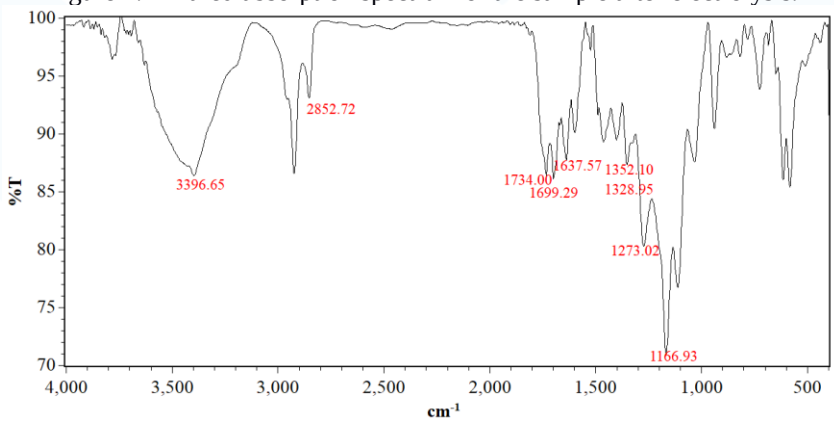

Source: Author

Table 3. Absorption frequencies and assignments of the main infrared absorption bands to the sample after electrolysis.

Wavenumber	Possible assignments [18,19]
3396.65*	O-H stretching (alcohol)
2852.72*	C-H stretching (aldehyde)

ISSN: 1696-8352

1734.00*	C=O axial stretching (aldehyde)
1699.29	C=O axial stretching (amide)
1637.57*	N-H bending (primary amine)
1352.10 e 1328.95	S=O asymmetric axial stretching (sulfone)
1273.02	C-N axial stretching (aromatic amine)
1166.93	S=O symmetric axial stretching (sulfone)

*Absorption bands absent in the LC infrared absorption spectrum.
Source: Author

The presence of a signal corresponding to the O-H stretch, in addition to the formation of bubbles with the addition of the LC solution, indicate the breaking of the carbonate bridge, just as it occurs in the human organism (Glina et al, 2009). However, the signal corresponding to the hydroxyl group from alcohol together with the presence of a band close to the expected value for the N-H bending from primary amine corroborates the hypothesis of the amide group reduction, in a similar way to that proposed by Largeron *et al.* (1997).

There is also an absorption band at 1734 cm^{-1}, which may be due to the stretching of the carbonyl group from aldehyde, which in general generates an absorption band between 1740 cm^{-1} and 1720 cm^{-1}. Although there is an unsaturation in carbon α to the carbonyl, which causes a reduction in the frequency of absorption, there is also an electronegative atom attached to this same carbon. Thus, there is an increase in the frequency of absorption, so that the value of 1734 cm^{-1} can be considered within the expected for the absorption related to the stretching of the aldehyde carbonyl group. In addition, aldehydes generally have two absorption bands at 2830 cm^{-1} to 2695 cm^{-1}, not present in the spectrum. These absorptions are commonly attributed to Fermi resonance, with the second band appearing when there is a coupling between the axial deformation of the aldehyde C-H and the first harmonic of the angular deformation of the aldehyde C-H that absorbs close to 1390 cm^{-1}. Thus, not all aldehydes present these two absorption bands. It is also possible to observe the presence of the absorption band at 2852 cm^{-1}, which in this case is not superimposed on the other C-H absorption bands. This may be due to the axial deformation of C-H from aldehyde. This data is compatible with the intermediate product formation in the process of reducing the amide group (Pavia, et al, 2009; Silverstein, et al, 1991).

ISSN: 1696-8352

3.4 CHEMICAL-QUANTUM CALCULATIONS AND PROPOSED MECHANISM

To identify possible groups susceptible to reduction, chemical-quantum calculations were performed, which were also carried out to assess whether the information obtained by characterizing the electrolysis products is consistent with the chemical-quantum properties of the molecule. The energies provided by the ORCA software are given in Hartrees (Eh), 1 Eh = 27.2113834 Ev (Neese, 2012). Figure 8 shows the relaxed lodenafil structure, with the numbering adopted, and Table 4 shows the values of atomic charges in all atoms of the molecule, except hydrogen. The data obtained indicate that the atoms N15, N28, N21, O1, O2, and O3 were the ones that presented more negative charges, being the most susceptible to protonation in acidic medium. Atoms that have more positive atomic charges and therefore the most likely to receive electrons are in decreasing order: S18, C14, C17, C13, C8, C6, C29, and C9.

Figure 8. Relaxed lodenafil structure and atom numbering adopted.

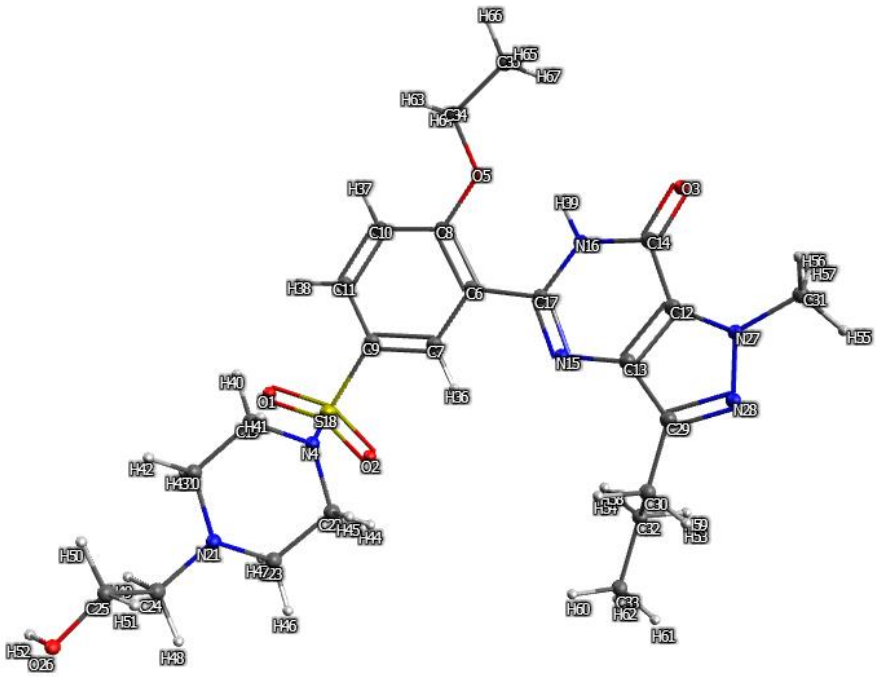

Source: Author

In addition to atomic charges, the analysis of the HOMO and LUMO orbitals is also important. The HOMO orbital corresponds to the last occupied molecular orbital,

ISSN: 1696-8352

therefore the most susceptible to lose electrons (oxidation). Thus, the more positive the energy of the HOMO orbitals, the more favorable is the possible oxidation reaction. The LUMO orbital corresponds to the first unoccupied molecular orbital, being the most susceptible to receiving electrons (reduction). Similarly, the more negative the energy of the LUMO orbitals, the more favorable the reduction reaction (Atkins, De Paula, 2010). Figure 9 graphically shows the HOMO and LUMO orbitals, where the colors were arbitrarily defined as red for HOMO (-) and LUMO (-) and blue for HOMO (+) and LUMO (+) orbitals.

Figure 9. HOMO and LUMO orbitals graphical representations for the lodenafil molecule. (a) Graphical representation of the HOMO orbital. (b) Graphical representation of the LUMO orbital.

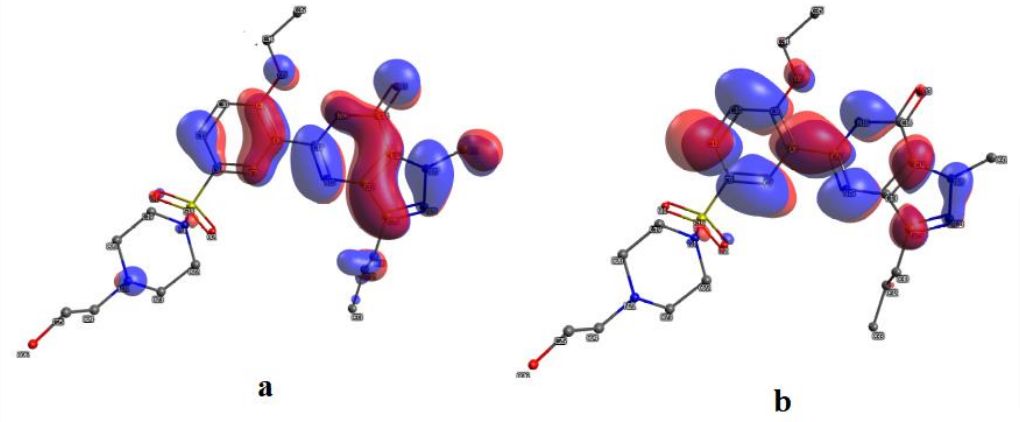

Source: Author.

Table 4. Quantum properties calculated for lodenafil.

Total Energy	**-1998.11550213 Eh**		
HOMO Energy	-0.21846 Eh		
LUMO Energy	-0.06805 Eh		
Charges on some atoms (except hydrogens) - Eh			
O 1	-0.632946	**C 19**	-0.235466
O 2	-0.635519	**C 20**	-0.129799
O 3	-0.541200	**N 21**	-0.278094
N 4	-0.313536	**C 22**	-0.079494
O 5	-0.454796	**C 23**	-0.109381
C 6	0.247586	**C 24**	-0.012701
C 7	-0.449279	**C 25**	0.001455
C 8	0.299905	**O 26**	-0.453238
C 9	0.194590	**N 27**	0.034566
C 10	-0.138629	**N 28**	-0.390991
C 11	-0.223645	**C 29**	0.206803
C 12	0.060176	**C 30**	-0.310097
C 13	0.357603	**C 31**	-0.232495

ISSN: 1696-8352

C 14	0,381660	**C 32**	-0.173078
N 15	-0.597430	**C 33**	-0.331348
N 16	-0.253438	**C 34**	-0.014118
C 17	0.369493	**C 35**	-0.341045
S 18	1.290931		

Source: Author

It can be observed that the atoms who contribute the most to the LUMO orbital are N15, N16, C12, and the aromatic ring carbons, it being more favorable for reduction reactions to occur in these atoms. It is worth mentioning that, as shown in Table 4, the energy of the LUMO orbital is negative, which favors reductions reactions. Note, too, that there is no contribution of a sulfur atom and little contribution given by oxygen atom (O3) to this orbital, which makes it difficult to reduce the sulfone group. However, there is a strong contribution given by nitrogen amide, favoring the reaction in this group or on nitrogen atoms N28 and N15, causing double bond saturation.

The data obtained by chronoamperometry and square wave voltammetry indicate that the LC reduction occurs with the consumption of 11 to 12 electrons. However, in an acidic medium, the LC molecule breaks down, releasing two molecules of lodenafil. Thus, the proposed mechanism must consider the lodenafil molecule and not the dimer, thus presenting a consumption of half the electrons compared to that consumed by the dimer.

The sulfone group reduction as the first process was discarded since no data were found to corroborate this hypothesis in the FT-IR spectra. Also, the chemical-quantum calculations show that although the S18 atom has the most positive charge density among the atoms of the molecule, which in theory would make it more susceptible to receiving electrons, the contribution of this region to the LUMO orbital is insignificant compared to the contribution given by the aromatic ring and by the amide and amine groups.

The product obtained after electrolysis showed characteristic bands of alcohol, primary amines, and aldehyde in the FTIR spectrum. These data corroborate the hypothesis that there is an amide group reduction to aldehyde, with the subsequent reduction of the aldehyde group to alcohol. Furthermore, it indicates that in the first stage a primary amine can also be generated, as described for pyridylcarboxamides reduction

ISSN: 1696-8352

(Largeron et al, 1997). Thus, it was proposed that first, the amide group reduction of the lodenafil molecule occurs, as shown in Figure 10.

Figure 10. Amide group reduction mechanism of the lodenafil molecule.

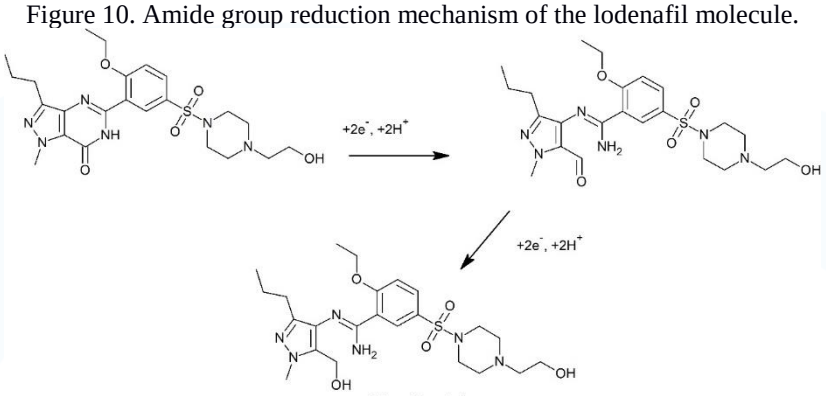

Source: Author

In this process, there is the consumption of four electrons, which explains part of the mechanism, but the data obtained by square wave voltammetry and chronoamperometry indicate a total number of six electrons consumed per lodenafil molecule. Then, chemical-quantum calculations were also performed with product 1, to identify where a reduction reaction is most likely to occur. Were proposed two possibilities: the first involves the sulfone group reduction and the second the unsaturated amine reduction. The product 1 relaxed structure with the adopted numbering is shown in Figure 11. Table 5 shows the atomic charges calculated for the main atoms, where it is possible to observe that the most negative electronic densities are on the atoms O1, O2, N15, and N28, which are susceptible to protonation. Therefore, it is consistent with the possibility of sulfone group reduction as well as the possibility of unsaturated amine group reduction. It is also observed that the atoms with more positive charge density are in decreasing order the S18, C17, C8, C6, C29, C13, C12, C9, N27, and C25, indicating that these are the most available to receive electrons.

Figure 11. Product 1 relaxed structure and numbering adopted.

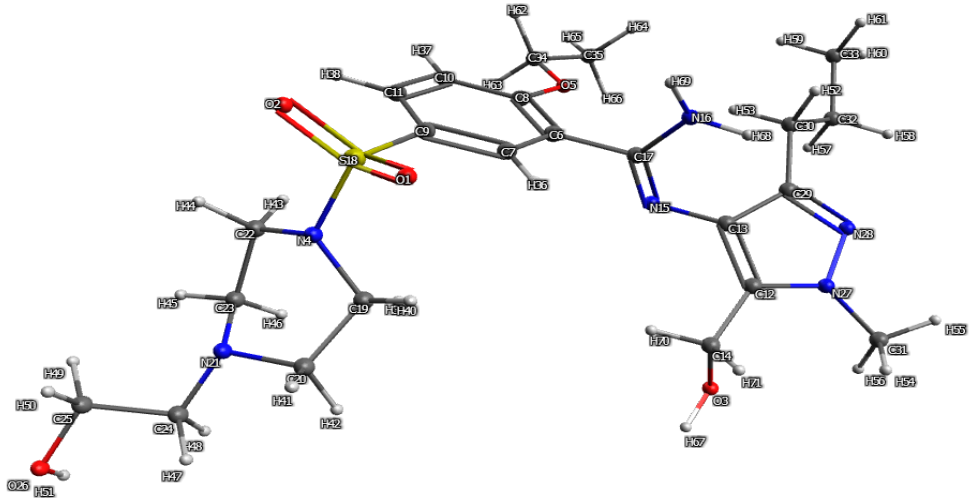

Source: Author

Table 5. Quantum properties calculated for product 1.

Total Energy	**-2000.46313125 Eh**		
HOMO Energy	-0.20309 Eh		
LUMO Energy	-0.03686 Eh		
Charges on some atoms (except hydrogens) - Eh			
O 1	-0.644799	**C 19**	-0.146083
O 2	-0.643934	**C 20**	-0.070186
O 3	-0.446188	**N 21**	-0.261717
N 4	-0.243648	**C 22**	-0.131048
O 5	-0.386304	**C 23**	-0.078580
C 6	0.267410	**C 24**	-0.080192
C 7	-0.462771	**C 25**	0.042313
C 8	0.315283	**O 26**	-0.456975
C 9	0.124000	**N 27**	0.071504
C 10	-0.187041	**N 28**	-0.438263
C 11	-0.254046	**C 29**	0.200127
C 12	0.138633	**C 30**	-0.319055
C 13	0.185708	**C 31**	-0.225953
C 14	-0.161224	**C 32**	-0.100399
N 15	-0.570660	**C 33**	-0.339664
N 16	-0.453087	**C 34**	-0.013742
C 17	0.522185	**C 35**	-0.339067
S 18	1.335973		

Source: Author

Note, that the energy value of the LUMO orbital for Product 1 is equal to - 0.03686 Eh (Table 5), being more positive than the energy found for the LUMO orbital of the lodenafil molecule -0.06805 Eh (Table 4). This value indicates that the potential necessary to the product 1 reduction tends to be less than that needed to reduce the

lodenafil molecule so that its reduction probably occurs at a more negative potential than lodenafil reduction (Atkins, De Paula, 2010).

Figure 12 shows the HOMO and LUMO orbitals for product 1. The colors were arbitrarily defined as red HOMO (-) and LUMO (-) and blue the HOMO (+) and LUMO (+) orbitals. Note that the atoms that contribute most to the LUMO orbital are those belonging to the 6-membered aromatic ring, in addition to the N15 and N16 nitrogen, which would favor the reduction of the unsaturation present in the N15 atom. In addition, there is no contribution given to the LUMO orbital by nitrogen N28, which hinders a reaction to reduce the unsaturation present in this atom. There is also a significant contribution to the LUMO orbital given by the atoms of the sulfone group and in α position to this one, which are the atoms S18, O1, O2, C9, and N4. This also indicates that a reduction process can occur in this group. The data obtained by chemical-quantum calculations allow us to say that the reduction of unsaturation present in atom N28 is unlikely. However, it indicates that both the reduction of the sulfone group and the reduction of unsaturation present in atom N15 can occur. Furthermore, it is possible to observe a significant contribution to the LUMO orbital given by the atoms of the sulfone group and in α position to this one, which are the atoms S18, O1, O2, C9, and N4. This also indicates that a reduction process can occur in this group. The data obtained by chemical-quantum calculations allow us to say that the reduction of unsaturation present in atom N28 is unlikely. However, it indicates that both the sulfone group reduction and the reduction of unsaturation present in atom N15 can occur.

Figure 12. HOMO and LUMO orbitals graphical representations for the product 1. (a) Graphical representation of the HOMO orbital. (b) Graphical representation of the LUMO orbital.

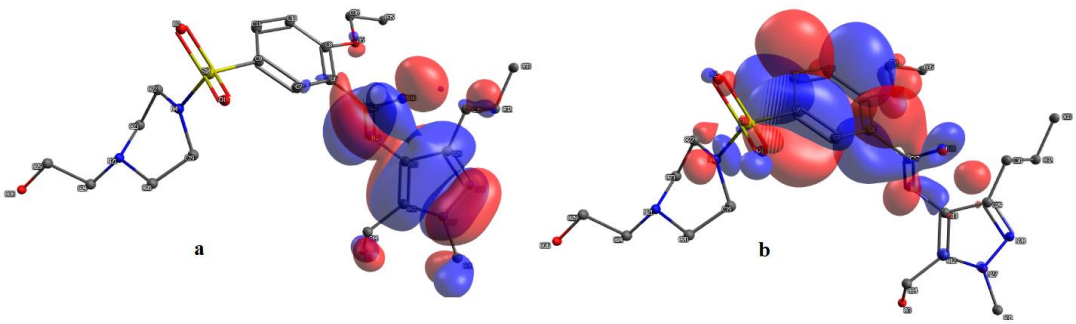

Source: Author

ISSN: 1696-8352

Given the above, it is suggested that after the amide group reduction to primary alcohol and amine, two more reduction processes may occur. One possibility is that the saturated amine (N15 atom) is reduced (Hammerich, Speiser, 2016). Another fact that corroborates this hypothesis is that such a reduction process occurs with the formation of an unstable radical, which quickly reacts, causing it not to be detected at a lower scan rate. This justifies the last peak present in the square wave voltammetry, which is only perceptible in the cyclic voltammetry at scan rates greater than 150 mV s^{-1} (Figure 2). The other hypothesis is the reduction of the sulfone group, which also occurs with a radical formation. This data is also consistent with the behavior observed in the voltammetric techniques employed (Coeffard, 2008).

Figure 13 shows the proposed mechanism for lodenafil reduction on HMDE, in the first step the amide group is reduced to primary amine and aldehyde. Subsequent reduction of the aldehyde group to primary alcohol occurs, forming intermediate product 1, which is reduced by a new process involving two electrons. However, for this second process, it was not possible to determine which path would be more favorable to undergo reduction, if A or B.

Figure 13. Proposed mechanism for lodenafil reduction in acidic media.

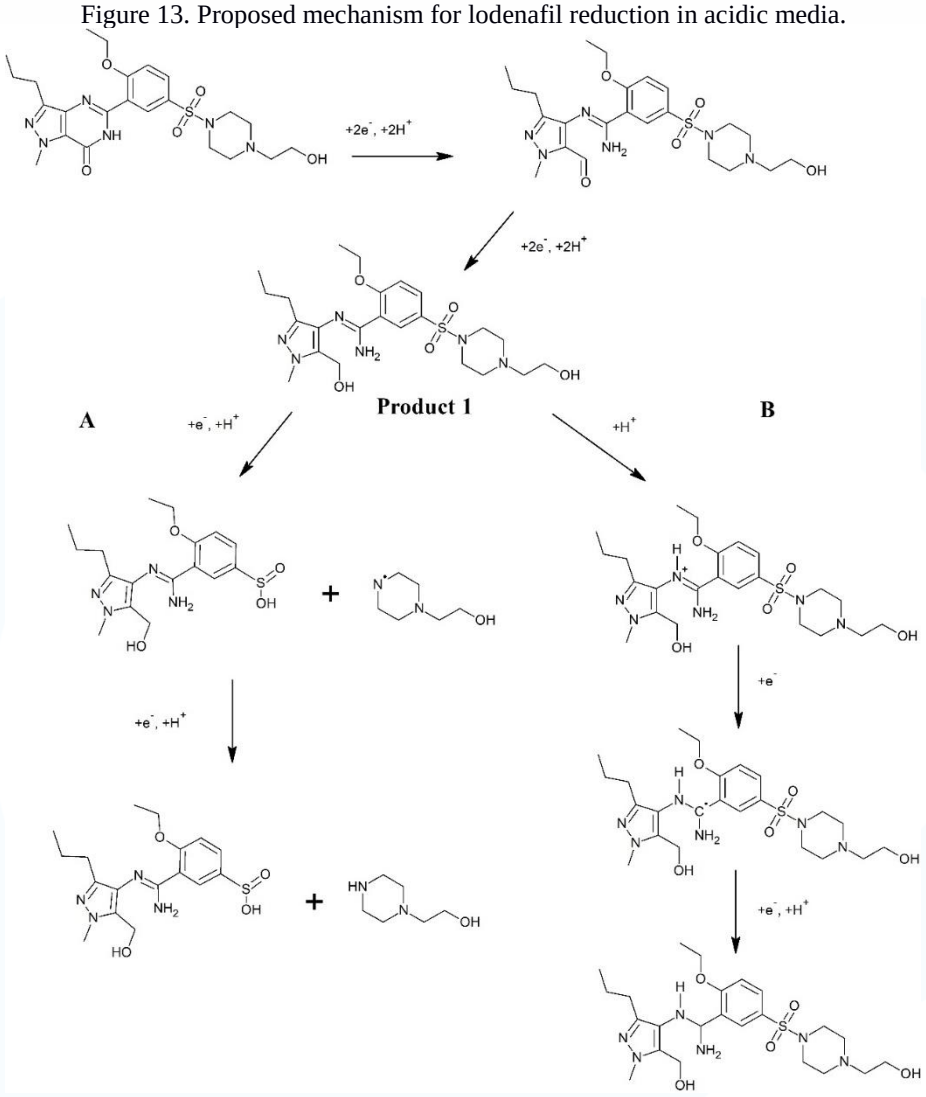

Source: Author

4 CONCLUSIONS

The results obtained show that the LC reduction mechanism in acid medium is complex since it involves four irreversible reduction processes, one of which has a radical character. The study of this reaction mechanism by voltammetry and chronoamperometry, in addition to characterizations by FT-IR, and chemical-quantum calculations, provided information that allowed us to propose a mechanism for lodenafil reduction. The amide group reduction to aldehyde was established, which was later reduced to an alcohol, with a consumption of four electrons. However, voltammetric and chronoamperometric data suggested the consumption of six electrons per molecule. Thus,

ISSN: 1696-8352

two possible routes have been proposed to occur with the product formed in the previous step, namely the sulfone group reduction and the reduction of the azomethine adjacent to the six-membered aromatic ring. The electrochemical, spectroscopic and computational data were in accordance with the occurrence of all the processes. However, in the second stage where there is the consumption of two electrons, it was not possible to establish which one would be the most favorable if the reduction of the sulfone group or the reduction of azomethine.

ACKNOWLEDGMENTS

"This study was financed in part by the Coordenação de Aperfeiçoamento de Pessoal de Nível Superior - Brasil (CAPES) - Finance Code 001". The authors would like to thank Cristália Produtos Farmacêuticos for kindly donating the LC standard. J.S.C thanks CAPES for the Master's scholarship. S.P.Q thanks CNPq for its research productivity grant.

ISSN: 1696-8352

REFERENCES

Alshehri, Y. M., Al-Majed, A. A., Attwa, M. W., Bakheit, A. H. (2022) Lodenafil in : Profiles of Drug Substances, Excipients and Related Methodology. Volume 47, 2022, Chapter Four, 113-147.

Atkins, P., De Paula, J. (2010) Physical Chemistry, Vol. 1, Oxford University Press, p. 944.

Avogadro: an open-source molecular builder and visualization tool. Version 1.2.0. access in January 2023. http://avogadro.cc/

Bard, A. J., Faulkner, L. R. (2001) Electrochemical Methods Fundamentals And Applications, JOHN WILEY & SONS, INC., New York, p. 833.

Berzas, J. J., Rodriguez, J., Castañeda, G., Villaseñor, M. J. (2000) Voltammetric behavior of sildenafil citrate (Viagra) using square wave and adsorptive stripping square wave techniques determination in pharmaceutical products. ***Analytica Chimica Acta.*** 417, 143–148. doi:https://doi.org/10.1016/S0003-2670(00)00932-6

Brett, A. M. O., Brett, C. M. A. (1993) Electrochemistry: principles, methods and applications, Oxford University, Coimbra, p. 464.

Codevilla, C. F., Castilhos, T. S., Bergold, A. M. (2013) A review of analytical methods for the determination of four new phosphodiesterase type 5 inhibitors in biological samples and pharmaceutical preparations, ***Brazilian Journal Of Pharmaceutical Sciences,*** 49, 1-11. doi:http://dx.doi.org/10.1590/S1984-82502013000100002

Coeffard, V.,Thobic-Gautier, C., Beaudet, I., Le Grognec, E., Quintard, J. P. (2008) Mild Electrochemical Deprotection of N-Phenylsulfonyl N-Substituted Amines Derived from (R)-Phenylglycinol, *European Journal of Organic Chemistry.* 383–391. doi:https://doi.org/10.1002/ejoc.200700709

Davis, J. E., Nunes,K. P., Stallmann-Jorgensen, I., Webb, R. C. (2012) Current Perspectives on Pharmacotherapy Treatments for Erectile Dysfunction, In: K. P. Nunes (Ed.), **Erectile Dysfunction - Disease-Associated Mechanisms and Novel Insights into Therapy**, Ch. 8, Intech,, p. 145-160.

Galli, A., Caetano,J. C., Homem-de-mello, P., Silva, A. B. F.,Ferreira, A. G., Almeida, S. V., Machado, S. A. S. (2018) A mechanistic study of the electrochemical behavior of pendimethalin herbicide. ***Journal Of Electroanalytical Chemistry.*** 826, 157-163. doi:https://doi.org/10.1016/j.jelechem.2018.08.038

Glina, S., Toscano, I., Gomatzky, C., De Góes, P. M., Júnior, A. N., Claro, J. F. A., Pagani, E. (2009) Efficacy and tolerability of lodenafil carbonate for oral therapy in

erectile dysfunction: a phase II clinical trial, *J Sex Med* . 6, 553-557. doi:https://doi.org/10.1111/j.1743-6109.2008.01079.x

Gosser-Junior, K. D. (1993) Cyclic Voltammetry: simulation and analysis of reaction mechanisms, VCH, New York, p. 154.

Hammerich, O., Speiser, B. (2016) Organic electrochemistry**,** CRC Press, p. 1776.

Han, W. S., Hong, J. Y., Hong, J. K., Kim, J. H., Kim, J. K., Lee, Y. H., Hong, T. K. (2012) Electrochemical Behavior of Udenafil on Glass Carbon Electrode, *J. of the Korea Society for Environmental Analysis.* 61-66.

Hanwell, M. D., Curtis, D. E., Lonie, D. C., Vandermeersch, T., Zurek, E., Hutchison, G. R. (2012) Avogadro: An advanced semantic chemical editor, visualization, and analysis platform, *Journal of Cheminformatics.* 4-17. https://doi.org/10.1186/1758-2946-4-17

Largeron, M., Auzeil, N., Bacqué, E., Fleury, M. B. (1997) Influence of steric crowding on the electrochemical reduction of substituted tertiary pyridylcarboxamides in aqueous acidic medium, *Journal of the Chemical Society*, Perkin Transactions 2, 495-502.

Marrani,A. G., Motta, A., Schrebler,R., Zanoni, R., Dalchiele, E. A. (2019) Insights from experiment and theory into the electrochemical reduction mechanism of graphene oxide, *Electrochimica Acta.* 304, 231-238. https://doi.org/10.1016/j.electacta.2019.02.108

Neese, F. The ORCA program system, (2012) *Comput. Mol. Sci*. 2, 73–78. doi:https://doi.org/10.1002/wcms.81

Pavia, D. L., Lampman, G. M., Kriz, G. S., Vyvyan, J. R. (2009) Introduction to spectroscopy, Cengage Learning, p. 752.
Scaglione, F., Donde, S., Hassan, T. A., Jannini, E. A. (2017) Phosphodiesterase Type 5 Inhibitors for the Treatment of Erectile Dysfunction: Pharmacology and Clinical Impact of the Sildenafil Citrate Orodispersible Tablet Formulation, ***Clinical Therapeutics.*** 39, 370-377. doi:http://dx.doi.org/10.1016/j.clinthera.2017.01.001

Silverstein, R. M., Bassler, G. C., Morrill, T. C. (1991) Spectrometric Identification of Organic Compounds. John Wiley & Sons, p. 430.

Skoog, A. D., West, D. M., Holler, F. J., Crouch, R. S. (2013) Fundamentals of Analytical Chemistry, Cengage Learning, p. 1072.

Souza, D., Machado, S. A. S., Avaca, L. A. (2003) Square wave voltammetry. Part I: theoretical aspects. *Química Nova.* 26, 81-89. doi:http://dx.doi.org/10.1590/S0100-40422003000100015

ISSN: 1696-8352

Uslu, B., Dogan, B., Ozkan, S. A., Aboul-Enein, H. Y., (2005) Electrochemical behavior of vardenafil on glassy carbon electrode: Determination in tablets and human serum. *Analytica Chimica Acta.* 552, 127-134. doi:http://dx.doi.org/10.1016/j.aca.2005.07.040
Wang, J. Analytical electrochemistry (2006) WILEY VCH, New Jersey, p. 250.

ISSN: 1696-8352

ANNEXES

Fig. S1**:** Dependence between peak current intensity and scan rate for a LC solution (0.700 µmol L^{-1}).

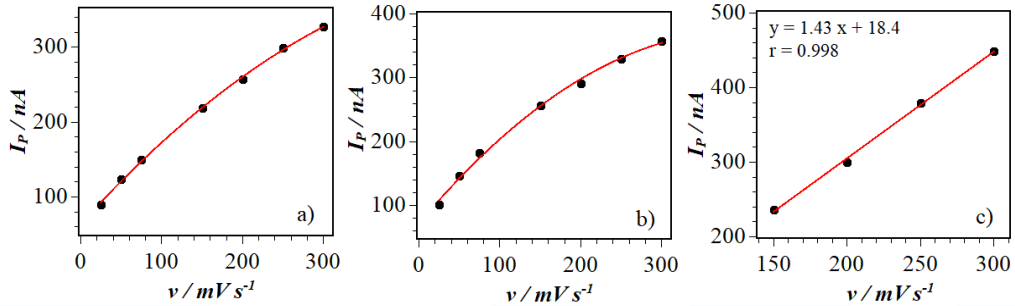

a) Peak 1 (-0.9 V). b) Peak 2 (-1.0 V). c) Peak 3 (-1.1 V). Cyclic voltammetry conditions: E_{ac} -0.8 V; t_{ac} 30 s; t_{eq} 10 s; ΔE_s 6 mV s^{-1}.
Source: Author

Fig. S2: Dependence between peak current intensity logarithm and scan rate logarithm for a LC solution (0.700 µmol L^{-1}).

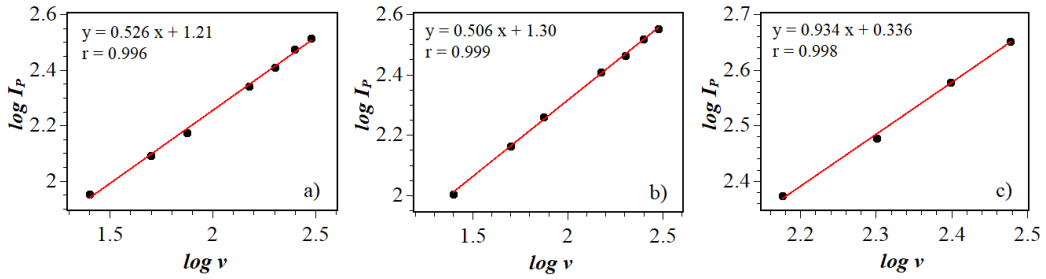

a) Peak 1 (-0.9 V). b) Peak 2 (-1.0 V). c) Peak 3 (-1.1 V). Cyclic voltammetry conditions: E_{ac} -0.8 V; t_{ac} 30 s; t_{eq} 10 s; ΔE_s 6 mV s^{-1}.
Source: Author

Fig. S3**:** Dependence between peak current intensity as a function of the square root of the scan rate for an LC solution (0.700 µmol L^{-1}).

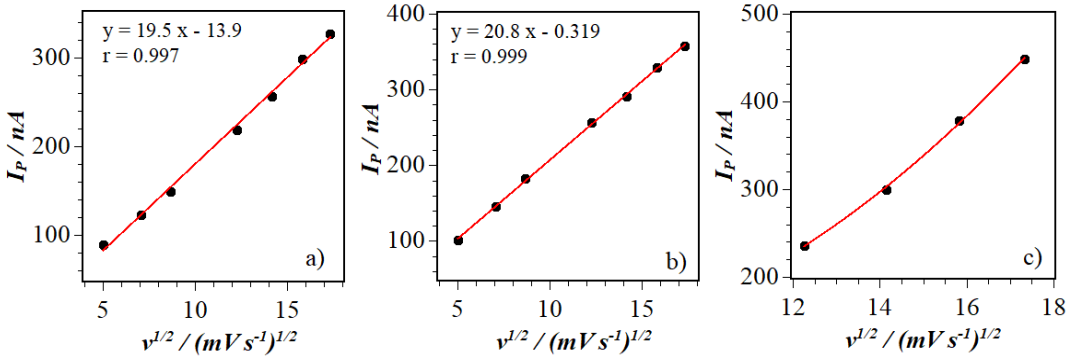

a) Peak 1 (-0.9 V). b) Peak 2 (-1.0 V). c) Peak 3 (-1.1 V). Cyclic voltammetry conditions: E_{ac} -0.8 V; t_{ac} 30 s; t_{eq} 10 s; ΔE_s 6 mV s^{-1}.
Source: Author